A NUMERICAL ANALYSIS OF FINITE DISPLACEMENT PROBLEMS OF ELASTIC SHELL STRUCTURES

By Takamasa SAKURAI*, Kazuo CHU** and Fumio NISHINO***

A formulation of geometrical nonlinear problems of shells with particular emphasis on the treatment of finite rotations is presented. The finite rotations are deleted in the formulation by removing them and hence only infinitesimally small rotations appear in the formulation. The deformed shell surface is given with the help of interpolation functions by the position vectors and by normal and tangential vectors of the surface at the nodes. A few numerical examples on shallow spherical shells are presented to compare the numerical results with the experimental results.

1. INTRODUCTION

Structural analyses are mostly carried out by discretizing the governing equation and solving the resulting algebraic equations. In finite displacement structural analyses, a standard procedure is to formulate the governing equation by using the so-called Lagrangian approach, i. e., the deformed shape is described by a coordinate system defined at the initial undeformed state. The approach may be divided into two. The first is to employ the same coordinates throughout analyses, whereas the second approach employs transformed coordinates of the original coordinates to avoid appearance of finite displacements and rotations in the governing equations by removing rigid body movement. Both of them, however, are the same in the sense that the coordinates are defined at the initial state. Following Goto et al. [1], the former is called as the direct Lagrangian approach and the latter as the Lagrangian approach with removal of rigid body motion. The governing equations may also be classified into two: the total Lagrangian formulation and the incremental or up-dated Lagrangian formulation.

In finite displacement analyses of space structures, it is inevitable to treat finite rotations and displacements. Both of them have to be evaluated to the same accuracy for the analyses to be accurate and reliable. Finite rotations are not vectors and naturally do not follow operational rules of vectors. This causes additional difficulty unlike finite displacements which are vectors[2]. Special attention has to be paid to treat finite rotations in the finite displacement analyses of three dimensional structures including shells.

The total Lagrangian approach does not involve any accumulated errors when numerical solutions satisfying the governing equations are obtained. It seems, however, that no reports based on the total

* Associate Professor, Department of Civil Engineering, Toyota College of Technology, Toyota-shi, Aichi-Ken, 471 Japan.
** Research Associate, Department of Civil Engineering, Toyota College of Technology, Toyota-shi, Aichi-Ken, 471 Japan.
*** Vice-president for Academic Affairs, Asian Institute of Technology, Bangkok, Thailand, on leave from University of Tokyo.

Lagrangian approach of the finite displacement analyses;of shells have yet been presented on the problems where finite rotations are treated rigorously.

The Lagrangian approach with removal of rigid body motion can eliminate higher order terms in the strain-displacement relation provided strain remains infinitesimally small. The procedure is proved to give rigorous solution of finite displacement problems in the case of plane frames[1]. The approach has been incorporated with the incremental formulation and been used to obtain numerical solutions on plate and shell problems[3].

The total Lagrangian formulation is superior to the incremental formulation for two reasons. Firstly, solutions can be obtained directly without any accumulation of error regardless of loading increments and, secondly, it can treat the geometrical boundary conditions of finite magnitudes without any complexity. The latter could be more important.

This paper persents an additional contribution to the finite displacement analyses of shells. The total Lagrangian method is employed in the formulation of governing equations, in which the finite rotations are not employed as the basic unknowns; instead the small difference between principal vectors of the surfaces at nodes and the points close to the nodes are used as basic unknowns to treat the finite rotations rigorously. Numerical solutions are obtained by solving discretized algebraic governing equations obtained by the finite element technique utilizing the successive approximation equivalent to the Newton-Raphson iteration[4]. Shell surfaces are approximated by a combination of small triangular plate elements. Equilibrium paths are traced solving the governing equations.

2. STRAIN-POSITION RELATIONS OF THIN PLATES

Define Cartesian coordinates fixed in space with base vectors $<I_1 \ I_2 \ I_3>$. Its origin is denoted by O_0 as shown in **Fig. 1**. Two arbitrary points on the middle plane of a plate element at the initial stress free undeformed state are denoted by O and P and the same points in the deformed equilibrium state by $\hat{O}$ and $\hat{P}$. The position vectors of $\hat{O}$ and $\hat{P}$ with the origin at O_0 are denoted by $\hat{X}^o$ and $\hat{X}^p$. The position vector of P with origin at O are denoted by x^p and that of $\hat{P}$ with the origin at $\hat{O}$ by $\hat{x}^p$. The vectors $\hat{X}^p, \hat{X}^o$ and $\hat{x}^p$ are related as

$$\hat{X}^p = \hat{X}^0 + \hat{x}^p \quad\quad\quad\quad\quad (1)$$

Fig. 1   Coordinate System of a Representative Shell Element E.

For a plate element at the initial state, orthogonal right handed unit vectors $<i_{o1} \ i_{o2} \ i_{o3}>$ are selected in such a way that i_{o3} is the normal vector to the middle surface. Similar orthogonal unit vectors $<i_1 \ i_2 \ i_3>$ are defined in the same way at the deformed state on the tangential plane at the middle surface of an arbitrary selected point $\hat{O}$ inside the element. Define scalar components of the vector x^p decomposed by i_{oa} by x^p_α as

$$x^p = x^p_\alpha i_{o\alpha} \quad (\alpha = 1, 2) \quad\quad\quad\quad\quad\quad\quad\quad\quad\quad\quad\quad (2)$$

The components of the position vectors at the deformed state are defined by decomposing by i_i as

$$\hat{X}^p = \hat{X}^p_i i_i, \quad \hat{X}^o = \hat{X}^o_i i_i, \quad \hat{x}^p = \hat{x}^p_i i_i \quad\quad\quad\quad\quad\quad\quad (3 \cdot a \sim c)$$

The vectors i_i are expressed by the vector I_i as

$$i_i = l_{ij} I_j \quad\quad\quad\quad\quad\quad\quad\quad\quad\quad\quad\quad\quad\quad\quad\quad\quad\quad (4)$$

where l_{ij}=direction cosines between the vectors i_i, and the vector I_j, respectively. The Roman and Greek subscripts such as i, j and α, β take $(1, 2, 3)$ and $(1, 2)$, respectively, unless otherwise stated in the rest of this paper. Summation convention is used for repeated subscripts in Eqs. (2) ~ (4) and is used also in the rest of the paper.

Designating the base vector at $\hat{P}$ on the middle surface of a plate element at the deformed state by
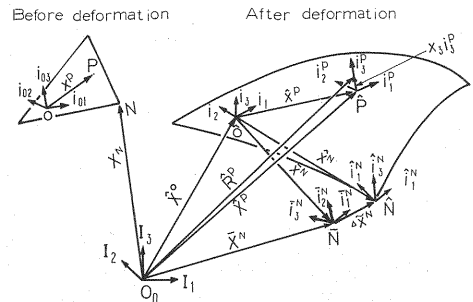
$a_\alpha^p(0)$, where (0) indicates the value at the middle surface, i. e. at $x_3=0$, and noting the definition of base vectors and the fact that $\hat{X}^o$ is independent of independent variable x_i^p, Eq. (1) and Eq. (3·c) yields

$$a_\alpha^p(0)=\hat{X}_{,\alpha}^p=\hat{x}_{i,\alpha}^p i_i \cdots\cdots\cdots\cdots\cdots\cdots\cdots\cdots\cdots\cdots\cdots\cdots\cdots\cdots\cdots\cdots\cdots\cdots\cdots\cdots (5\cdot a)$$

where $(\ )_{,\alpha}=(\ )/\partial x_\alpha^p$. The unit normal at $\hat{P}$ is given by its definition as

$$a_3^p(0)=[a_1^p(0)\times a_2^p(0)]/|a_1^p(0)\times a_2^p(0)| \cdots\cdots\cdots\cdots\cdots\cdots\cdots\cdots\cdots\cdots\cdots (5\cdot b)$$

where $(\times)=$cross product of vectors. Substituting Eq. (5·a) into Eq. (5·b) and neglecting the 2nd and higher order terms of $(\hat{x}_i^p-x_i^p)_{,\alpha}$ which corresponds to the derivatives of i-th component of a displacement vector, result in

$$a_3^p(0)=i_3-\hat{x}_{3,\gamma}^p i_\gamma \cdots\cdots\cdots\cdots\cdots\cdots\cdots\cdots\cdots\cdots\cdots\cdots\cdots\cdots\cdots\cdots\cdots\cdots\cdots\cdots\cdots\cdots (6)$$

Designating the normal distance including the sense from the middle surface at $\hat{P}$ by x_3 and the position vector of this point at x_3 with the origin at O_o by $\hat{R}^p$, it is expressed as

$$\hat{R}^p=\hat{X}^p+x_3 a_3^p(0) \cdots\cdots\cdots\cdots\cdots\cdots\cdots\cdots\cdots\cdots\cdots\cdots\cdots\cdots\cdots\cdots\cdots\cdots\cdots\cdots\cdots (7)$$

Using Eqs. (5·a) and (7), the base vector $a_\alpha^p(x_3)$ at point x_3 on the normal from P is given as

$$a_\alpha^p(x_3)=\hat{R}_{,\alpha}^p=a_{,\alpha}^p(0)+x_3 a_{3,\alpha}^p(0) \cdots\cdots\cdots\cdots\cdots\cdots\cdots\cdots\cdots\cdots\cdots\cdots\cdots (8)$$

Designating Green's strain tensor on the surface at point x_3 by $\varepsilon_{\alpha\beta}$, it is defined as

$$\varepsilon_{\alpha\beta}=[a_{\alpha\beta}^p(x_3)-\delta_{\alpha\beta}]/2 \cdots\cdots\cdots\cdots\cdots\cdots\cdots\cdots\cdots\cdots\cdots\cdots\cdots\cdots\cdots\cdots\cdots (9\cdot a)$$

where $\delta_{\alpha\beta}=$Kronecker's delta and $a_{\alpha\beta}^p(x_3)$ is a metric tensor at x_3 as defined by

$$a_{\alpha\beta}^p(x_3)=a_\alpha^p(x_3)\cdot a_\beta^p(x_3) \cdots\cdots\cdots\cdots\cdots\cdots\cdots\cdots\cdots\cdots\cdots\cdots\cdots\cdots\cdots\cdots\cdots (9\cdot b)$$

where $(\cdot)$ means scalar product. Neglecting small quantities of higher orders in view of the hypothesis of Kirchhoff and Love and the assumption of no change of thickness, the strain tensor is given from Eqs. (6), (8) and (9·a) as

$$\varepsilon_{\alpha\beta}=\eta_{\alpha\beta}+x_3\chi_{\alpha\beta} \cdots\cdots\cdots\cdots\cdots\cdots\cdots\cdots\cdots\cdots\cdots\cdots\cdots\cdots\cdots\cdots\cdots\cdots\cdots (10\cdot a)$$

Noting the assumption of small strain i. e. the absolute magnitude of strain is much smaller than unity, and using the relation of Eq. (9·a), $\eta_{\alpha\beta}$ and $\chi_{\alpha\beta}$ of Eq. (10·a) are expressed as

$$\eta_{\alpha\beta}=[(\hat{x}_\alpha^p-x_\alpha^p)_{,\beta}+(\hat{x}_\beta^p-x_\beta^p)_{,\alpha}+\hat{x}_{3,\alpha}^p\hat{x}_{3,\beta}^p+(\hat{x}_\gamma^p-x_\gamma^p)_{,\alpha}(\hat{x}_\gamma^p-x_\gamma^p)_{,\beta}]/2 \cdots\cdots (10\cdot b)$$

$$\chi_{\alpha\beta}=-\hat{x}_{3,\alpha\beta}^p+\hat{x}_{3,\gamma}^p\hat{x}_{\gamma,\alpha\beta}^p \cdots\cdots\cdots\cdots\cdots\cdots\cdots\cdots\cdots\cdots\cdots\cdots\cdots\cdots\cdots\cdots (10\cdot c)$$

The remaining tensor components $\varepsilon_{3\alpha}$, $\varepsilon_{\alpha3}$, and ε_{33} are all identically equal to zero due to Kirchhoff and Love hypothesis and the assumption of no thickness change.

With the assumption of small strain, the angles between the base vectors at any points on the middle surface of shells are no longer right angles because of shear strain, however, the change of angles is of small quantity with respect to unity. Axial strains are also of small quantities by the same assumption. Because of these facts, it is possible to select orthogonal unit vectors $i_\alpha(\alpha=1,2)$ to satisfy

$$i_\alpha\approx a_\alpha^o(0) \cdots\cdots\cdots\cdots\cdots\cdots\cdots\cdots\cdots\cdots\cdots\cdots\cdots\cdots\cdots\cdots\cdots\cdots\cdots\cdots\cdots\cdots\cdots\cdots (11\cdot a)$$

in the tangential plane at the point $\hat{O}$ as shown in **Fig. 1**. Since the normal vector at this point, $a_3^o(0)$, is a unit vector, the unit vector i_3 orthogonal to i_α coincides with $a_3^o(0)$ as

$$i_3=a_3^o(0) \cdots\cdots\cdots\cdots\cdots\cdots\cdots\cdots\cdots\cdots\cdots\cdots\cdots\cdots\cdots\cdots\cdots\cdots\cdots\cdots\cdots\cdots\cdots\cdots\cdots (11\cdot b)$$

This orthogonal set of unit vectors, $<i_1\ i_2\ i_3>$, as defined in Eq. (11) are called in this paper as principal vectors of an element. The values of components of the position vector of P with respect of O, x_β^p, do not change when the plane moves with rigid body motion to a new plane on which i_α is defined. In view of this fact, the Taylor expansion of $a_\alpha^p(0)$ as expressed in Eq. (5) at the point $\hat{O}$ up to the second order term can be expressed as

$$a_\alpha^p(0)\approx i_\alpha+\hat{x}_{i,\alpha\beta}^o x_\beta^p i_i \cdots\cdots\cdots\cdots\cdots\cdots\cdots\cdots\cdots\cdots\cdots\cdots\cdots\cdots\cdots\cdots\cdots (12\cdot a)$$

Similarly, the normal base vector at the point $\hat{P}$, $a_3^p(0)$, is expressed, in view of Eq. (6) as

$$a_3^p(0)\approx i_3-\hat{x}_{3,\gamma\beta}^o x_\beta^p i_\gamma \cdots\cdots\cdots\cdots\cdots\cdots\cdots\cdots\cdots\cdots\cdots\cdots\cdots\cdots\cdots\cdots\cdots (12\cdot b)$$

Eq. (12) shows that, under the assumption of small strain, x_β^p can be made as small as necessary by selecting the small element and hence the base vectors $a_i^p(0)$ at an arbitrary point inside the small element can be expressed as

$$a_i^p(0) = i_i + Q_{ij}(\varepsilon) i_j \quad \cdots\cdots\cdots\cdots\cdots\cdots\cdots\cdots\cdots\cdots\cdots\cdots\cdots\cdots (13)$$

where $Q_{ij}(\varepsilon)$=small quantity of the order of strain. Similar to the selection of i_i at $\hat{O}$, select orthogonal unit vectors i_α^p and i_3^p in the tangential plane at the point $\hat{P}$ as close to the base vectors $a_\alpha^p(0)$ and $a_3^p(0)$ at the same point. These vectors are called as the principal vectors at the point $\hat{P}$. Because of the selection of i_i and i_i^p inside a small element, the angle between the coresponding vectors i_i and i_i^p is small quantity and hence this angle can be treated as a vector. This rotation vector at $\hat{P}$ between i_i^p and i_i are defined as $\hat{\theta}^p$ which can be decomposed by i_i as

$$\hat{\theta}^p = \hat{\theta}_i^p i_i \quad \cdots\cdots\cdots\cdots\cdots\cdots\cdots\cdots\cdots\cdots\cdots\cdots\cdots\cdots\cdots\cdots\cdots\cdots\cdots\cdots\cdots\cdots\cdots (14)$$

where $\hat{\theta}_i^p$=rotation vector of i_i to coincide with i_i^p.

Since the principal vectors of an element is selected to satisfy Eq. (11), the square of the term $(\hat{x}_\gamma^p - x_\gamma^p)_{,\alpha}$ as present in Eq. (10·b), is of the order of the square of strains and hence can be neglected as a small quantity with respect to the first order term. In numerical analyses, use of either the exact expression or only linear terms in Eqs. (10·b, c) results in exact solutions, when iteration converges[1),4)]. It is reported, however, in analyses of plane frames that the maximum convergence is expected when only the third term of Eq. (10·b) is retained rather than retaining all second order terms[1)]. In order to detect critical points on the equilibrium paths, representative second order nonlinear terms have to be retained in Eq. (10). Because of these reasons, only the third term of Eq. (10·b) is retained among the second order terms in the analyses of this paper. This treatment coincides with von Karman's nonlinear finite displacement plate theory. The strain-displacement relations to be employed in the following analyses are summarized as

$$\eta_{\alpha\beta} = \eta_{\alpha\beta}^l + \eta_{\alpha\beta}^{nl}, \quad \varkappa_{\alpha\beta} = \varkappa_{\alpha\beta}^l \quad \cdots\cdots\cdots\cdots\cdots\cdots\cdots\cdots\cdots\cdots\cdots\cdots (15\cdot a, b)$$

where

$$\eta_{\alpha\beta}^l = [(\hat{x}_\alpha^p - x_\alpha^p)_{,\beta} + (\hat{x}_\beta^p - x_\beta^p)_{,\alpha}]/2, \quad \eta_{\alpha\beta}^{nl} = \hat{x}_{3,\alpha}^p \hat{x}_{3,\beta}^p/2, \quad \varkappa_{\alpha\beta}^l = -\hat{x}_{3,\alpha\beta}^p \quad \cdots\cdots\cdots (15\cdot c\sim e)$$

3.   STIFFNESS EQUATION AND BOUNDARY CONDITIONS

Consider a nodal point $\hat{N}$ of the element E as shown in Fig. 1. The position vector of this point with the origin at $\hat{O}$ is designated by $\hat{x}^N$. Similar to the definition of rotation vector $\hat{\theta}^p$ defined in relation to Eq. (14), the small rotation vector of the point $\hat{N}$ in relation to the orthogonal unit vector i_i defined at $\hat{O}$ is denoted by $\hat{\theta}^N$. These two vectors are decomposed by the orthogonal unit vectors defined at $\hat{O}$ as

$$\hat{x}^N = \hat{x}_i^N i_i, \quad \hat{\theta}^N = \hat{\theta}_i^N i_i \quad \cdots\cdots\cdots\cdots\cdots\cdots\cdots\cdots\cdots\cdots\cdots\cdots\cdots\cdots (16\cdot a, b)$$

All components of $\hat{x}^N$ and $\hat{\theta}^N$ in one element E are designated by $\hat{\boldsymbol{\delta}}_E$. In view of Eq. (16), it is expressed for 3 nodes triangular plate element as

$$\hat{\boldsymbol{\delta}}_E = \langle \hat{x}_i^N \ \hat{\theta}_i^N \rangle_E^T \quad (i, N=1, 2, 3) \quad \cdots\cdots\cdots\cdots\cdots\cdots\cdots\cdots\cdots\cdots (17)$$

where superscript T=transpose of a matrix.

Consider as external forces, only the forces act at nodes. The forces acting at a node $\hat{N}$ are divided into the force vector designated by N^N and the moment vector designated by M^N. Decomposing them by i_i leads

$$N^N = \hat{N}_i^N i_i, \quad M^N = \hat{M}_i^N i_i \quad \cdots\cdots\cdots\cdots\cdots\cdots\cdots\cdots\cdots\cdots\cdots\cdots\cdots (18\cdot a, b)$$

Similar to Eq. (17), all components of $\hat{N}_i^N$ and $\hat{M}_i^N$ in one element are designated by $\hat{F}_E$, then

$$\hat{F}_E = \langle \hat{N}_i^N \ \hat{M}_i^N \rangle_E^T \quad (i, N=1, 2, 3) \quad \cdots\cdots\cdots\cdots\cdots\cdots\cdots\cdots\cdots\cdots (19)$$

Utilizing the standard finite element discretization procedure with algebraic interpolation functions as stated later leads to the stiffness equation for the element in terms of components of the principal vectors of the element i_i defined at $\hat{O}$ as

$$\hat{F}_E = \hat{K}_E \hat{\boldsymbol{\delta}}_E + \hat{C}_E \quad \cdots\cdots\cdots\cdots\cdots\cdots\cdots\cdots\cdots\cdots\cdots\cdots\cdots\cdots\cdots\cdots\cdots (20)$$

where $\hat{K}_E = \hat{K}_E^l + \hat{K}_E^{nl}$ element stiffness matrix; and $\hat{C}_E$=term appearing dur to the use of position vectors $\hat{\boldsymbol{\delta}}_E$ as a basic unknown at nodes rather than displacement vectors[4)]. It is noted that all components in $\hat{F}_E$ and $\hat{\boldsymbol{\delta}}_E$ are vector quantities. As obvious from the description, the position of $\hat{O}$ and its principal directions have to be fixed to evaluate the terms of Eq. (20).

The transformation matrix T_E from the global coordinate defined at O_o to the orthogonal unit base vectors at $\hat{O}$ of the element E is defined as

$$\{i_i\} = T_E\{I_i\} \quad \cdots\cdots\cdots\cdots\cdots\cdots\cdots\cdots\cdots\cdots\cdots\cdots\cdots\cdots\cdots\cdots\cdots (21)$$

By utilizing this transformation matrix the stiffness equation, Eq. (20), can be transformed to the stiffness equation with the components in global base vectors as

$$\tilde{F}_E = \tilde{K}_E \tilde{\delta}_E + \tilde{C}_E \quad \cdots\cdots\cdots\cdots\cdots\cdots\cdots\cdots\cdots\cdots\cdots\cdots\cdots (22)$$

where $\quad \tilde{F}_E = \hat{T}_E^T \hat{F}_E, \quad \tilde{\delta}_E = \hat{T}_E^T \hat{\delta}_E, \quad \tilde{C}_E = \hat{T}_E^T \hat{C}_E, \quad \tilde{K}_E = \hat{T}_E^T \hat{K}_E \hat{T}_E \quad \cdots\cdots\cdots\cdots (23 \cdot a \sim d)$

$$\hat{T}_E = \begin{bmatrix} T_E^N & & 0 \\ & T_E^N & \\ 0 & & T_E^N \end{bmatrix}, \quad T_E^N = \begin{bmatrix} T_E & 0 \\ 0 & T_E \end{bmatrix} \quad \cdots\cdots\cdots\cdots\cdots\cdots (24 \cdot a, b)$$

Since the nodal point $\hat{N}$ at the deformed equilibrium state is unknown, an arbitrary point near the guessed position of $\hat{N}$ is selected as the N-th node and is named as $\overline{N}$ as shown in Fig. 1. This point $\overline{N}$ is treated as the common node of all elements meeting at the same point. The principal base vectors $<\overline{i}_1^N \; \overline{i}_2^N \; \overline{i}_3^N>$ and $<\hat{i}_1^N \; \hat{i}_2^N \; \hat{i}_3^N>$ are defined at $\overline{N}$ and $\hat{N}$ in the same way as i_i^p as defined at $\hat{P}$. Expressing the unknown but possibly small position vector from $\overline{N}$ to $\hat{N}$ by $\Delta \tilde{x}^N$ and unknown small rotation vector necessary to match $\overline{i}_i^N$ to $\hat{i}_i^N$ by $\Delta \tilde{\theta}^N$, they are given by

$$\Delta \tilde{x}^N = \hat{x}^N - \overline{x}^N, \quad \Delta \tilde{\theta}^N = \hat{\theta}^N - \overline{\theta}^N \quad \cdots\cdots\cdots\cdots\cdots\cdots\cdots\cdots (25 \cdot a, b)$$

where $\overline{x}^N =$ position vector from $\hat{O}$ to $\overline{N}$ and $\overline{\theta}^N =$ small rotation vectors defined at $\overline{N}$ in the same way as for $\hat{\theta}^p$ at $\hat{P}$. Decomposing the above vectors by global base vectors I_i and utilizing these components, define

$$\Delta \tilde{\delta}_E = <\Delta \tilde{x}_i^N \; \Delta \tilde{\theta}_i^N>_E^T, \quad \overline{\delta}_E = <\overline{x}_i^N \; \overline{\theta}_i^N>_E^T \quad (i, N = 1, 2, 3) \quad \cdots\cdots\cdots (26), (27)$$

in the same way as for $\hat{\delta}_E$ of Eq. (17). Substituting Eq. (26) into Eq. (20) leads to

$$\tilde{F}_E = \tilde{K}_E \Delta \tilde{\delta}_E + \tilde{F}_{Eo} \quad \cdots\cdots\cdots\cdots\cdots\cdots\cdots\cdots\cdots\cdots\cdots\cdots (28)$$

where $\quad \tilde{F}_{Eo} = \tilde{K}_E \overline{\delta}_E + \tilde{C}_E \quad \cdots\cdots\cdots\cdots\cdots\cdots\cdots\cdots\cdots\cdots (29)$

Utilizing the equilibrium condition and continuity conditions at each node such as

$$\tilde{F}^N = \sum \tilde{F}_E^N, \quad \Delta \tilde{\delta}^N = \Delta \tilde{\delta}_E^N \quad (N = 1, 2 \text{ or } 3) \quad \cdots\cdots\cdots\cdots (30 \cdot a, b)$$

where $\tilde{F}^N$ is the external force vector at node $\hat{N}$, and $\Delta \tilde{\delta}^N$ is the difference of position and rotation vector between point $\hat{N}$ and $\overline{N}$, the total stiffness equation of shells is obtained in the following standard form

$$\tilde{F} = \tilde{K} \Delta \tilde{\delta} + \tilde{F}_o \quad \cdots\cdots\cdots\cdots\cdots\cdots\cdots\cdots\cdots\cdots\cdots\cdots\cdots (31)$$

When the solution $\Delta \tilde{\delta}$ becomes equal to zero, $\overline{N}$ coincides with $\hat{N}$. To obtain the solution $\Delta \tilde{\delta} = 0$ in Eq. (31), an iterative process is necessary. The unknowns in Eq. (31) are $\overline{\delta}_E$ as included in $\tilde{F}_o$ and $\Delta \tilde{\delta}$. To solve Eq. (31) for $\Delta \tilde{\delta}$, the components of $\overline{\delta}_E$ have to be assumed for each node of each element, i. e., the positions and the principal directions of both $\hat{O}$ and $\overline{N}$ for each element.

When $\Delta \tilde{\delta} = 0$ is obtained, the position of the node $\hat{N}$ of the element E is given by

$$\hat{X}^N = \hat{X}^o + \overline{x}^N \quad \cdots\cdots\cdots\cdots\cdots\cdots\cdots\cdots\cdots\cdots\cdots\cdots\cdots\cdots (32)$$

Similarly the principal directions of the same node are given, in view of Eq. (21) and the components of rotation vector of Eq. (27), as

$$\{\overline{i}_i^N\} = \tilde{T}^N \{\overline{I}_i^N\} \quad \cdots\cdots\cdots\cdots\cdots\cdots\cdots\cdots\cdots\cdots\cdots\cdots\cdots\cdots (33)$$

where $\tilde{T}^N = T_E \overline{T}^N \quad \cdots\cdots\cdots\cdots\cdots\cdots\cdots\cdots\cdots\cdots\cdots\cdots\cdots\cdots\cdots (34)$

and $\overline{T}^N$ is the transformation matrix from $(T_E)^{-1} i_i$ to $(T_E)^{-1} \overline{i}_i^N$ at $\overline{N}$ as given

$$\overline{T}^N = \begin{bmatrix} 1 & \overline{\theta}_3^N & -\overline{\theta}_2^N \\ -\overline{\theta}_3^N & 1 & \overline{\theta}_1^N \\ \overline{\theta}_2^N & -\overline{\theta}_1^N & 1 \end{bmatrix} \quad \cdots\cdots\cdots\cdots\cdots\cdots\cdots\cdots\cdots (35)$$

If angles of the principal directions of the node of the element E are necessary, they can be computed from

the components of the transformation matrix $\tilde{T}^N$, which are the direction cosines between the global base vectors and the principal vectors at the node $\hat{N}$ of the element.

Initial values play an important role in iteration. When a solution is known at one equilibrium point, the solution at the point or appropriately extrapolated values would be used as the initial values for the next solution. The selection of origin O in an element is arbitrary. It can be selected somewhere in the middle of the three nodes. As the initial values of the position of $\hat{O}$ and its principal directions and as these up-dated values for the succesive iteration, values close to the averages of the position and the directions of the three nodes may be selected .

The kinematic boundary conditions for the total stiffness equation expressed by Eq. (31) is specified by the given quantities of the components of the force vector $\tilde{F}$. The corresponding geometric boundary condition is given by specifying 0 values for the correspondign components of the vector $\Delta\tilde{\delta}$. Thus the boundary conditions are expressed as

$$\Delta\tilde{x}_j^N = 0 \quad \text{or} \quad \tilde{N}_j^N = \tilde{N}_j^{Ng} \quad \text{and} \quad \Delta\tilde{\theta}_j^N = 0 \quad \text{or} \quad \tilde{M}_j^N = \tilde{M}_j^{Ng} \cdots\cdots\cdots (36 \cdot a, b)$$

where $\Delta\tilde{x}_j^N$ and $\Delta\tilde{\theta}_j^N$ are the components of $\Delta\tilde{\delta}$ at $\hat{N}$ and $\tilde{N}_j^N$ and $\tilde{M}_j^N$ are the components of $\tilde{F}$ corresponding to $\Delta\tilde{x}_j$ and $\Delta\tilde{\theta}_j$, decomposed by the global base vectors. The superscript g shows given quantity.

4. NUMERICAL EXAMPLES

Numerical analyses of shells are performed by idealizing the shells by a combination of triangular flat plate elements. These idealized shells are discretized by the finite element technique[5] and the resulting nonlinear algebraic equations as expressed by Eq. (31) are solved by the method of successive approximation equivalent to the Newton-Raphson iteration[4].

For the derivation of elastic stiffness matrix $\hat{K}_E^l$ for a triangular element, the linear interpolation function with two degrees of freedom for a node is used for membrane and the third order polynomial with three degrees of freedom for a node and with three sub-elements is used for bending. With these interpolation functions, displacements between the elements are compatible. While for the derivation of geometric stiffness $\hat{K}_E^{nl}$ for bending, non displacement compatible third order polynomial interpolation function without any sub-element is used for the simplicity of derivation. Because of these degrees of freedom, the stiffness matrix $\hat{K}_E = \hat{K}_E^l + \hat{K}_E^{nl}$ has five degrees of freedom with respect to the coordinate defined for a flat plate element. Though there exists a report concerned on the freedom of the rigid body rotation of the element about the normal to the middle plane of the plate element[6], this rotation is not considered in the formulation of this report. By transforming five degrees of freedom at a node into a space coordinate, stiffness equations with six degrees of freedom at a node are formulated.

In tracing an equilibrium curve in $(n+1)$ dimensional space with n degrees of freedom of nodal positions and rotations, and loading intensity for a fixed loading pattern, n simultaneous stiffness equations are not sufficient. An additional condition needs to be specified, which is given by specifying loading intensity, one of n components of position or rotation vectors, or an increment of chord length from a known point of an equilibrium path[4]. In the numerical analyses of this report, one of the former two conditions is employed. The convergence of the solution is attained when the unknown vector $\Delta\tilde{\delta}$ approaches zero. Noting that the components of vectors $\Delta\tilde{x}^N$ and $\Delta\tilde{\theta}^N$ at each node $\overline{N}$ of a shell, the following conversion criterion K has been used

$$K = \frac{1}{M}\sum_{(N)}\left(k_x\frac{|\Delta\tilde{x}^N|}{|\overline{X}^N - X^N|} + k_\theta\frac{|\Delta\tilde{\theta}^N|}{|\overline{\theta}_o^N|}\right) < \varepsilon \cdots\cdots\cdots\cdots (37)$$

where M = total number of nodes ; $\sum_{(N)}$ = summation on all nodes ; k_x, k_θ = arbitrary convex weights on position and rotation vectors, respectively ; and ε = small quantity to measure the convergence. $\overline{X}^N - X^N$ and $\overline{\theta}_o^N$ are the displacement vector and the rotation vector between i_{oi} and $\overline{i}_i^N$, respectively.

Employing the strain tensors of Eqs. (15·c~e) as have been employed in the linearized finite

displacement theory under the action of in-plane initial stresses in the formulation of the stiffness equation of Eq. (20), the stiffness matrix $\hat{K}_E$ is expressed by the sum of two matrices as

$$\hat{K}_E = \hat{K}_E^l + \hat{K}_E^{nl} \quad\cdots\cdots\cdots\cdots\cdots\cdots\cdots\cdots\cdots\cdots\cdots\cdots\cdots\cdots\cdots\cdots\cdots\cdots\cdots\cdots\cdots\cdots\cdots\cdots\cdots\cdots\cdots \quad (38)$$

where $\hat{K}_E^l$ and $\hat{K}_E^{nl}$ are the matrices corresponding to the linear and the nonlinear terms, $\eta_{\alpha\beta}^l$ and $\chi_{\alpha\beta}^l$, and $\eta_{\alpha\beta}^{nl}$, respectively, of Eqs. (15·c~e) and are called as the elastic stiffness matrix and the geometric stiffness matrix.

In numerical analyses, even using

$$\hat{K}_E = \hat{K}_E^l \quad\cdots\cdots\cdots\cdots\cdots\cdots\cdots\cdots\cdots\cdots\cdots\cdots\cdots\cdots\cdots\cdots\cdots\cdots\cdots\cdots\cdots\cdots\cdots\cdots\cdots\cdots\cdots\cdots\cdots\cdots \quad (39)$$

results in the solution of the governing nonlinear equations, when the iteration converges. In the former case, the successive approximation becomes equivalent to the Newton-Raphson iteration[4]. Hence there is a convergence area near a solution. In the latter case, successive approximation is not equivalent to the Newton-Raphson procedure and hence there is no guarantee of convergence even the initial guess solution is selected close to the true solution[4].

Fig. 2 is the numerical results of a shell structure consisting with two flat plates of which one end is simply supported and the neighboring two pair edges are free under a concentrated load at the center of the structure as shown in the inserted figure. Numerical analyses are done only one quarter of the structure taking advantage of symmetry of the structure and the loading.

Considering the fact that convergence criterion on position vector includes the component of rigid body rotation of the element, the weights of $k_x = 1$ and $k_\theta = 0$ are employed. As the measure of convergence, ε of 0.01 is used. The small inserted figure shows the relationship between loading intensity P versus the vertical displacement δ at the loading point. The major figure of Fig. 2 shows the approach of the loading to the

Fig. 2 Convergence of Solutions versus Stiffness Matrix and Number of Elements.

true loading intensity with the increasing number of elements for the use of both stiffness matrix of Eqs. (38) and (39) when the vertical displacements of loading point is specified as 0.5 cm, 1 cm, and 1.5 cm as designated by ①, ②, and ③, respectively. Since the solutions with 72 elements and the stiffness matrix of Eq. (38) can be regarded as the closest to the true solutions, other solutions are compared with these solutions. In all cases, the increase of the number of elements reduces the errors. The difference by the use of stiffness matrix of Eqs. (38) and (39) is significant in the unstable point ③. These results agree with the results obtained for the analysis of a beam-column[1]. This agreement is natural by the reasons that both plates and beam-columns can be regarded as similar structures and that the stiffness matrix of Eq. (38) represents more closely the structural characteristic of plates than that of Eq. (39).

As can be seen in the derivation of Eq. (38), $\hat{K}_E^{nl}$ is the geometrix matrix for a plate after the rigid body motion of the plate element close to the final position with reference coordinate i_i. Hence the stiffness matrix $\hat{K}_E$ of Eq. (38) represents the tangential stiffness matrix at the position after the rigid body motion under the existence of an internal membrane force. In the formulation of the direct Lagrangian formulation, the tangential stiffness matrix is expressed with the sum of the stiffness matrix for the small displacement theory, the initial displacement matrix and the initial stress matrix, while, in the Lagrangian formulation based on the coordinate defined based on the state after rigid body motion, the displacement matrix vanishes in the expression of the tangential stiffness matrix. The derivation of Eq. (38) corresponds to the latter. Since Eq. (38) is derived with reference to the coordinate after the rigid body
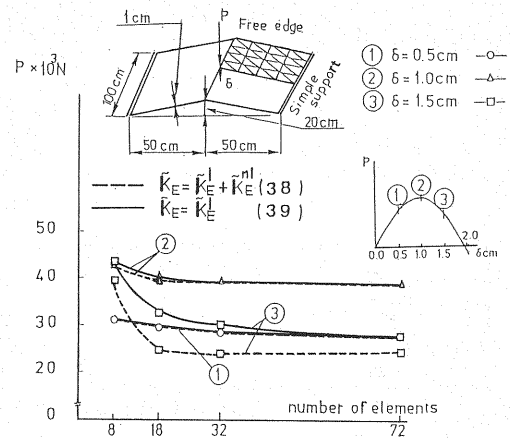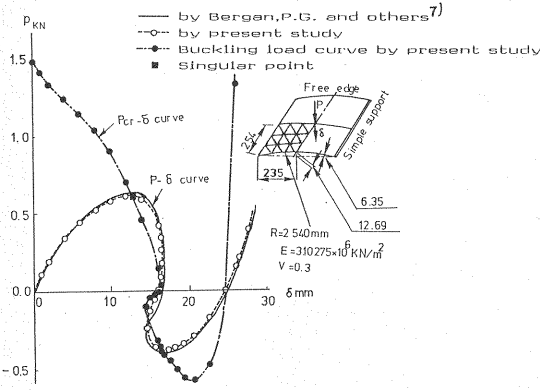
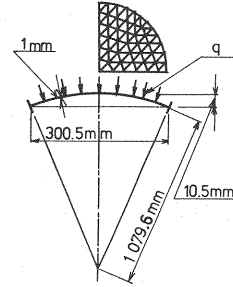Fig. 3 Equilibrium Paths and Buckling Load Curve.

Fig. 4 Spherical Shell.

motion under the existence of membrane force but no consideration is given for the presence of internal bending moments, it is not a rigorous tangential stiffness matrix but it is an approximate expression.

Considering proportional loading for simplicity, the nodal force vector $\tilde{F}$ in Eq. (31) is expressed by the product of loading intensity f and a vector $\tilde{f}$ specifying pattern as

$$\tilde{F} = f\tilde{f} \quad \cdots\cdots\cdots\cdots\cdots\cdots\cdots\cdots\cdots\cdots\cdots\cdots\cdots\cdots\cdots\cdots\cdots\cdots\cdots\cdots\cdots\cdots \quad (40)$$

The loading intensity of the critical load, λ, linearly extrapolated from the displaced state under the loading intensity f can be obtained by eigenvalue analysis of

$$[\tilde{K}^i + (\lambda/f)\tilde{K}^{nl}]\Delta\tilde{\delta} = 0 \quad \cdots\cdots\cdots\cdots\cdots\cdots\cdots\cdots\cdots\cdots\cdots\cdots\cdots\cdots\cdots\cdots \quad (41)$$

Fig. 3 shows the equilibrium path of the shell shown in the inserted figure. Numerical analyses are done on a quarter part of the shell dividing this part into 18 elements. The ordinate and abscissa are the loading intensity and the vertical displacement at the loading point, respectively. Also shown in the figure are the numerical results reported by Bergan et al[7]. These are the result using 50 triangular elements formulated using modified hybrid stress method. Both analyses agree reasonably well. The difference may be decreased by an increasing number of elements. The line with solid circles shows the critical loading intensity obtained by using the stiffness matrix of Eq. (38). The curve shows a significant decrease of the critical load with the progress of the displacement indicating the so-called bucking load evaluated based on the initial shape subjects to significant error in the evaluation of the true buckling load. At the maximum point of the loading intensity, the buckling load determined by Eq. (41) agrees with the maximum intensity obtained by tracing the equilibrium path by solving Eq. (31) within an error of one percent. This suggests that the error involved in the tangential matrix of Eq. (38) is very little even though the presence of internal bending moments is disregarded in the derivation of the initial stiffness matrix.

Numerical analyses and experimental results on domed shells under the uniformly distributed load perpendicular to the shell surface and fixed at the edges as shown in Fig. 4 are compared.

The specimens are made of aluminum alloys. The basic dimension of the specimen as well as the mesh arrangement for the numerical analyses are also shown in Fig. 4. The test on the material of the specimens resulted in Young's modulus $E = 7.22 \times 10^5$ kg/cm² (70.6 GN/m²) and Poisson's ratio $= 0.33$.

Fig. 5 shows numerical results for a perfect domed shell using the material properties obtained from the tests. The ordinate and abscissa show the intensity of uniform pressure, q, divided by the classical buckling intensity, q_{c1} obtained on the initial shape, and the vertical displacement at the crown nondimensionalized by the thickness of the shell. In the figure, n shows the number of buckling waves on a contour line. The loading intensities and the buckling modes at points A and B agree with the results reported by Huang[8]. It is well known that the experimentally obtained ultimate carrying capacity could be 1/4 to 3/4 of the classical buckling load. Yamada et al. has also confirmed this reduction[9].
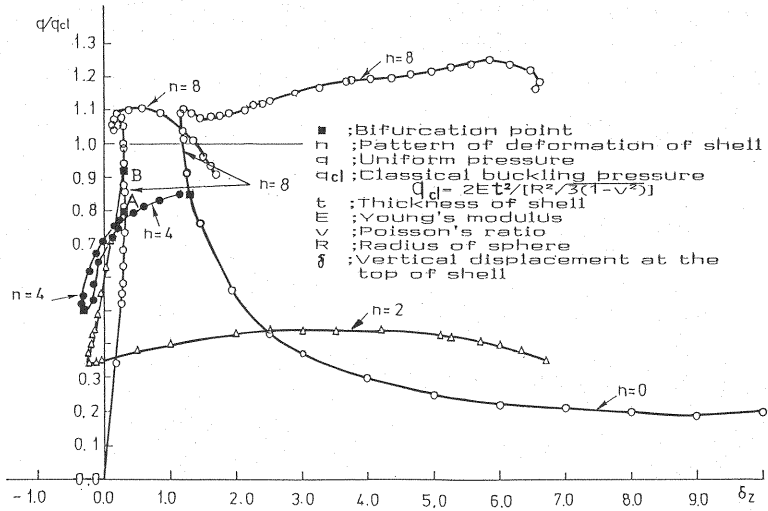
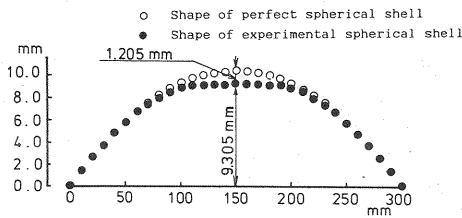Fig. 5 Equilibrium Paths for Perfect Spherical Shell.

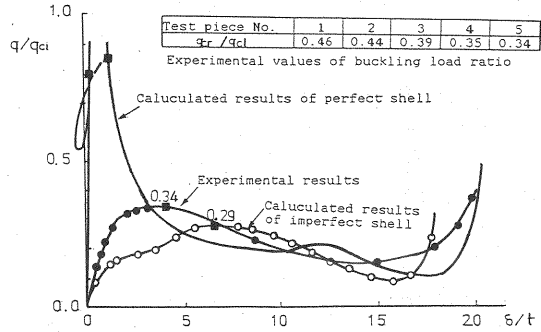Fig. 6 Initial Imperfection of Shell.

Fig. 7 Experiments versus Calculated Values.

Experiments has been performed on 5 specimens as shown in **Fig. 4**. The shape of one of the specimen was measured by using a 3-dimensional distance measuring instrument with an accuracy of 0.01 mm to determine the initial imperfection. The shape was mesured at 162 points on the 12 concentric circles. From these measurements, an axially symmetric imperfect shape of the dome is approximated by taking the average values of the points on the same contour lines. One of the results so determined is shown in **Fig. 6**. The standard deviation of the measurements of a height at a centerline is around 0.1 mm at the upper portion of the dome and around 0.2 mm at the lower portion. This specimen is named as the 5-th specimen.

Fig. 7 shows the pressure versus the displacement relationship at the top of the dome obtained by the experiment on the 5-th specimen and the numerical results on the dome with the measured geometrical shape as well as the numerical results for the perfect dome. The experimentally obtained maximum pressure exceeds the prediction by numerical analysis by 15 %. This difference could be due to the mechanical difference in the test set-up and the assumption made in the computation by taking the average values for the imperfection, and also due to the unavoidable error in the measurements of geometrical shape and limited number of points where measurements were made.

The experimentally obtained maximum pressures, q_{cr}, at the first peak of the pressure versus displacement relationships at the top of the dome are listed for all 5 specimens in the inserted table of **Fig. 7** in nondimensionalized form by the classical buckling pressure, q_{c1}, for the perfect dome.

The ratio between the critical pressure and the classical buckling pressure is roughly 0.8 for a perfect

dome, whereas the average of those ratios experimentally obtained for the 5 tests is 0.34. This fact confirms together with the results of numerical analyses that the presence of initial imperfections plays an important role in reducing the ultimate load carrying capacity from the classical buckling load.

5.   SUMMARY AND CONCLUDING REMARKS

The work is summarized as follows :

(1)   The displaced and deformed shape of shells is described by two orthogonal unit vectors on the tangential plane and a unit normal vector to it, and a position vector at each node of each element. To describe the shape with finite displacements and rotations, the above description is superior to the description by rotational angles and displacement vectors as used in most of the reports in literature by the reasons that the formulation is easier and rigorous and that the description of this work is irrelevant to the initial location of the element.

(2)   The nonlinear governing stiffness equation is formulated removing rigid body motion, i. e., by storing the large displacements and rotations outside the stiffness equation. With this procedure, the governing stiffness equation for the problems in which finite rotations occur is formulated without any terms related to finite rotations.

(3)   The stiffness matrix of Eq. 38 is nearly equal to the true tangential stiffness matrix with very small error. Singular points on equilibrium paths can be easily and accurately detected by performing eigenvalue analyses of the stiffness matrix when iteration converged.

ACKNOWLEDGEMENT

REFERENCES
1) Goto, Y., Hasegawa, A. and Nishino, F, : Accuracy of Finite Displacement Analysis of Plane Frames, Proc. of JSCE, No. 331, pp. 33~44, March 1984 (In Japanese).
2) Hayashi, M. and Maeda, Y. : Finite Displacement Analysis of Space Framed Structures, Proc. of JSCE, No. 253, pp. 13~27, September 1976 (In Japanese).
3) Yoshida, Y. and Masuda, N. and Matsuda, T. : A Discrete Element Approach to Elastic-Plastic Large Displacement Analysis of Thin Shell Structures, Proc. of JSCE, No. 288, pp. 41~55, August 1979 (In Japanese).
4) Nishino, F., Ikeda, K., Sakurai, T. and Hasegawa, A. : A Total Lagrangian Nonlinear Analysis of Elastic Trusses, Proc of JSCE, Structural Eng./Earthquake Eng., Vol. 1, No. 1, pp. 1 s~15 s, April 1984.
5) Bathe, K. J., Wilson, E. L. and Peterson, F. E. : SAP IV A Structural Analysis Program for Static and Dynamic Response of Linear Systems, A Report to the National Science Foundation, Report No. EERC 73-11, June 1973.
6) Suzuki, T. and Kaneko, H. : A Large Deflection Analysis for Buckling and Postbuckling Behavior of Plate Elements of Structural Members by the Finite Element Method, Transactions of the Architectural Institute of Japan, No. 316, pp. 9~16, June 1982 (In Japanese).
7) Bergan, P. G., Horrigmoe, G., Krakelard, B. and Soreide, T. H. : Solution Techniques for Nonlinear Finite Element Problems, Int. J. for Num. Meth. in Eng., Vol. 12, pp. 1677~1696, 1978.
8) Hung, N. : Unsymmetrical Buckling of Thin Shallow Spherical Shell, Journal of Applied Mechanics, Vol. 31, No. 3, pp. 447~457, September 1964.
9) Yamada, S., Uchiyama, K. and Yamada, M. : Experimental Investigation of the Buckling of Shallow Spherical Shells, Int. J. for Nonlinear Mech. Vol. 18, No. 1, pp. 37 ~54, 1983.